Available online at www.sciencedirect.com
SCIENCE DIRECT®
Journal of Computational Physics 205 (2005) 357–372
JOURNAL OF COMPUTATIONAL PHYSICS
www.elsevier.com/locate/jcp

Electrical impedance tomography using level set representation and total variational regularization

Eric T. Chung [a], Tony F. Chan [a], Xue-Cheng Tai [b,*]

[a] Department of Mathematics, University of California, Los Angeles, CA 90095-1555, USA
[b] Department of Mathematics, University of Bergen, Johnnes Brunsgate 12, N-5007 Bergen, Norway

Received 22 March 2004; received in revised form 18 October 2004; accepted 17 November 2004
Available online 19 December 2004

Abstract

In this paper, we propose a numerical scheme for the identification of piecewise constant conductivity coefficient for a problem arising from electrical impedance tomography. The key feature of the scheme is the use of level set method for the representation of interface between domains with different values of coefficients. Numerical tests show that our method can recover sharp interfaces and can tolerate a relatively high level of noise in the observation data. Results concerning the effects of number of measurements, noise level in the data as well as the regularization parameters on the accuracy of the scheme are also given.

1. Introduction

Electrical impedance tomography is a widely investigated problem with many applications in physical and biological sciences. It is well known that the inverse problem is nonlinear and highly ill-posed. Various numerical techniques with different advantages have been proposed to solve the problem. We begin by first giving a precise mathematical model for electrical impedance tomography. Let Ω be a bounded domain in $\mathbb{R}^2$ with C^1 boundary $\partial\Omega$ having outward normal n. We assume Ω contains material with electrical conductivity $q(x)$ satisfying $q(x) \geqslant q_0 > 0$. Then, the electrical potential $u(x)$ inside Ω satisfies

$$-\nabla \cdot (q\nabla u) = 0 \quad \text{in } \Omega, \tag{1}$$

$$q\frac{\partial u}{\partial n} = f \quad \text{on } \partial\Omega, \tag{2}$$

* Corresponding author. Fax: +47 55 58 96 72.
E-mail addresses: tschung@math.ucla.edu (E.T. Chung), chan@math.ucla.edu (T.F. Chan), tai@mi.uib.no (X.-C. Tai).

0021-9991/$ - see front matter © 2004 Published by Elsevier Inc.
doi:10.1016/j.jcp.2004.11.022

where $f(x)$ is the applied current density on $\partial\Omega$ such that the following conservation of charge relation holds:

$$\int_{\partial\Omega} f(s)\,\mathrm{d}s = 0.$$

The problem of electrical impedance tomography is to determine the electrical conductivity $q(x)$ inside Ω using a set of given values of applied current density $f(x)$ on $\partial\Omega$ and the corresponding observed values of electrical potential $u(x)$ on $\partial\Omega$. Such a mathematical model is obtained from Maxwell's equation under some conditions. See [10,32,35] for some more details about the derivation of the above model.

There are many efficient numerical techniques for solving the inverse problem, see [16,18–20,23,24,33,37,38]. For instance, in [11], a method called NOSER was proposed. The idea is to minimize the L^2-norm of the difference between the electrical potential due to the applied current and the measured potential on $\partial\Omega$. A one step Newton's method, with constant conductivity as initial guess, is employed to solve the minimization problem. The advantage is that most of the calculations, including the gradient of the functional to be minimized, can be done analytically. For other numerical approaches, we would like to mention some two-dimensional results for real data of Siltanen et al. [33]. These results showed the possibility of using electrical impedance tomography for real applications. For two-phase problems, the monotonicity method of [37,38] seems to be rather efficient and accurate. For a survey on these methods, see [10,25]. A problem that is related to electrical impedance tomography and is commonly solved in geophysics is called DC resistivity inverse problem. The only difference between the DC resistivity and the impedance tomography is that the data in DC resistivity are collected only on part of the boundary of the domain. Some reference of interest are [12,21,26,34]. To some extent, the DC resistivity is a relatively mature area and that unlike impedance tomography it is used on a daily basis for the detection of minerals and contaminated cites.

Brühl and Hanke [4] proposed a method based on an explicit criterion of whether a point is lying inside or outside of a certain set to solve the impedance tomography. Thus, a region with certain conductivity value can be reconstructed by testing every point in the computational domain. There is no need to minimize any functional, which means that there is no need to solve the forward problem numerically, as is normally required to perform many times when computing the gradient of the corresponding functional. Results of their experiments show that the method produces reasonably accuracy in most cases for noise level up to 1%. A theoretical justification of the numerical scheme has been given in [3].

Recently, the Mumford–Shah functional, which is a popular tool in image processing, was extended to the electrical impedance tomography problem in [31]. In addition to minimizing the L^2-norm of the difference between the potential due to the applied current and the measured potential, the L^2-norm of the gradient of the conductivity outside a discontinuity set and the Hausdorff measure of the discontinuity set are used as penalization terms. The conductivity coefficient is assumed to be known in a narrow region near the domain boundary. With presence of 1% of noise in the data, both the material interface and coefficient values can be accurately recovered. Besides numerical results, theoretical analysis of the numerical scheme is also given in [31]. See also [1,13,14,32] for some related studies for the same problem.

The level set idea, first proposed in [30], is known to be a powerful and versatile tool to model evolution of interfaces. The idea has also been used successfully in the context of inverse problem. The pioneering work of Osher and Santosa [29] uses the level set method for an inverse problem associated with shape optimization for the eigenvalues of the Laplace equation. In [17], the idea has been employed to solve an inverse conductivity problem. Assuming known conductivity values, the unknown conductivity interface can be solved by using values of Neumann data as well as values of solution in a thin layer along the boundary of a domain. In [8], the level set idea has been applied to solve elliptic inverse problems, where the unknown discontinuous coefficient has to be solved without the knowledge of both the values of the coefficient and

interfaces between the regions having different coefficient values. By using the value of solution or the gradient of solution of the forward problem in the domain, the coefficient can be accurately identified by utilizing the level set method. In [15], level set method has also been applied to solve an electromagnetic tomography problem with the model given by the Helmholtz equation. With known conductivity values, the interfaces of different materials are determined by using level set representation of curves. The work by Ameur et al. [2] treats a geometrical inverse problem using the level set methods. They try to recover a crack inside an elastic body from just one boundary measurement. See [5–7,27] for level set methods for other inverse problems.

In this paper, we will propose a method based on the level set idea to solve the inverse problem arising from electrical impedance tomography. We will consider the case where the electrical conductivity $q(x)$ is a piecewise constant function, with the possibility that the conductivity values are unknown. Following Chan and Tai [8,9] and Vese and Chan [39], we will represent the conductivity by using level set functions. With the representation of $q(x)$, we then solve the inverse problem by minimizing the L^2-norm of the difference between the potential due to the applied current and the measured potential on $\partial\Omega$. Since the minimization problem is highly ill-posed, we introduce a regularization using the total variation norm of $q(x)$ as in [9]. The choice of the regularization term allows the method to recover a sharp interface between different regions having different conductivity values. Moreover, it has been shown numerically that our method can tolerate relatively higher level of noise in the data.

This paper is organized as follows. In Section 2, we will give a brief overview of the level set method. We will present the use of level set functions to represent a piecewise constant function. Then, we will derive our method for solving the tomography problem by minimizing the L^2-error with total variation regularization. In Section 3, a series of numerical experiments is presented. We will show numerically that our method is able to recover simultaneously the unknown interface and the coefficient values. Also, we will discuss the sensitivity of our method with respect to number of observations, noise level and regularization parameter.

2. Numerical solutions to the inverse problem

For simplicity of presentation, we assume Ω contains two different materials with piecewise constant conductivities q_1 and q_2, where q_1 and q_2 are two positive real numbers. Let Ω_i be the region containing material with conductivity q_i ($i = 1,2$) and Γ be the interface between the two regions. Then, $q(x)$ can be represented as

$$q(x) = q_1 H(\phi(x)) + q_2(1 - H(\phi(x))) \quad \text{in } \Omega, \tag{3}$$

where $H(x)$ is the Heaviside function, namely

$$H(x) = 1 \quad \text{for } x \geqslant 0, \qquad H(x) = 0 \quad \text{for } x < 0,$$

and $\phi(x)$ is the level set function satisfying

$$\Omega_1 = \{x \in \Omega | \phi(x) > 0\},$$
$$\Omega_2 = \{x \in \Omega | \phi(x) < 0\},$$
$$\Gamma = \{x \in \Omega | \phi(x) = 0\}.$$

To determine the material interface Γ, it suffices to determine the level set function ϕ. It is clear that many different level set functions can achieve the above requirement. We will employ a signed distance function defined by

$$\phi(x) = \begin{cases} d(x,\Gamma) & \text{if } x \in \Omega_1, \\ -d(x,\Gamma) & \text{if } x \in \Omega_2. \end{cases} \tag{4}$$

It is clear that ϕ satisfies the partial differential equation

$$|\nabla\phi| = 1 \quad \text{in } \Omega. \tag{5}$$

However, ϕ is not the only solution to (5) in the sense of distribution. The unique solution to (5) is defined in the sense of viscosity solution. Let $\tilde{\phi}$ be any level set function that is positive inside Ω_1 and negative outside Ω_1. Then, the viscosity solution to (5) is defined as the unique steady state solution to

$$\frac{\partial d}{\partial t} + \operatorname{sign}(d)(|\nabla d| - 1) = 0, \quad d(x,0) = \tilde{\phi}. \tag{6}$$

See [28] for details. We shall mention that there are some variants of the level set methods which could avoid the use of the distance function and the Heaviside function H, see [22,36] for some details. Applying idea from Vese and Chan [39], we can extend the level set function representation of $q(x)$ in (3) in the case where the domain Ω contains more than two materials. Hence, our method, which will be derived for two unknown conductivity values, can be easily generalized to recover more than two conductivity values and their interfaces. The number of unknown conductivity values need not be specified, only the upper bound is needed. The redundant regions will disappear or merge with other regions during the iterative process. See also [8].

Let N be the number of measurements made. For $1 \leqslant i \leqslant N$, we let $f_i(x)$ be a given function representing a known applied current density on $\partial\Omega$ and $m_i(x)$ be the corresponding measurement of the electrical potential on $\partial\Omega$. We also denote by $u_i(x,q)$ the theoretical value of the electrical potential on Ω due to $f_i(x)$, where we emphasis the dependence of u_i on $q(x)$. Since the solution to the Neumann problem (1), (2) is not unique, we impose the following constraint on $u_i(x,q)$:

$$\int_{\partial\Omega} u_i(x,q)\,\mathrm{d}x = 0,$$

which means a ground state potential is specified. In order to find q_1, q_2, and the location of Γ, we minimize the following functional:

$$F(\phi, q_1, q_2) = \frac{1}{2}\sum_{i=1}^{N}\int_{\partial\Omega} |u_i(s,q) - m_i(s)|^2\,\mathrm{d}s.$$

Since the minimization problem is highly ill-posed, we will introduce a regularization term in the functional. Our choice is the total variation regularization, namely, we will find the minimum of the following functional:

$$F(\phi, q_1, q_2) = \frac{1}{2}\sum_{i=1}^{N}\int_{\partial\Omega} |u_i(s,q) - m_i(s)|^2\,\mathrm{d}s + \beta\int_{\Omega}|\nabla q|\,\mathrm{d}x, \tag{7}$$

where β is a regularization parameter to be chosen and

$$\int_{\Omega}|\nabla q|\,\mathrm{d}x$$

is the total variational norm of q (cf. [42]). The key of our numerical scheme is that the choice of total variation regularization ensures that both the jumps of coefficient values and the lengths of interfaces are controlled. See also [40]. This is different from the standard level set technique, which only controls the length.

We notice that F defined in (7) is a functional of q which again is a function of ϕ, q_1 and q_2. So, in order to compute the gradient of $F(\phi,q_1,q_2)$, we need to evaluate the gradient of F with respect to q as well as the differentials of q with respect to ϕ, q_1 and q_2, respectively. The gradient of F with respect to q is given by

$$\frac{\mathrm{d}F}{\mathrm{d}q} = -\sum_{i=1}^{N} \nabla u_i \cdot \nabla z_i - \beta \nabla \cdot \left(\frac{\nabla q}{|\nabla q|} \right), \tag{8}$$

where z_i ($i = 1,2,\ldots,N$) is the solution to the following problem

$$-\nabla \cdot (q \nabla z_i) = 0 \quad \text{in } \Omega,$$
$$q \frac{\partial z_i}{\partial n} = u_i - m_i \quad \text{on } \partial\Omega,$$

with the constraint

$$\int_{\partial\Omega} z_i(x)\, \mathrm{d}x = 0.$$

The first term on the right-hand side of (8) is the gradient with respect to q of the first term on the right-hand side of (7). The second term on the right-hand side of (8) is the gradient with respect to q of the second term on the right-hand side of (7). Using variational arguments, it can be shown that the following equality must be valid on the boundary if (ϕ, q_1, q_2) is a minimizer of (7)

$$\beta |\nabla q|^{-1} \frac{\partial q}{\partial n} = 0 \quad \text{on } \partial\Omega.$$

By the chain rule, we have (cf. [8, p. 45])

$$\frac{\mathrm{d}F}{\mathrm{d}\phi} = \frac{\mathrm{d}F}{\mathrm{d}q}\frac{\mathrm{d}q}{\mathrm{d}\phi} = \frac{\mathrm{d}F}{\mathrm{d}q}(q_1 - q_2)\delta(\phi), \tag{9}$$

$$\frac{\mathrm{d}F}{\mathrm{d}q_1} = \int_\Omega \frac{\mathrm{d}F}{\mathrm{d}q}\frac{\mathrm{d}q}{\mathrm{d}q_1}\,\mathrm{d}x = \int_\Omega \frac{\mathrm{d}F}{\mathrm{d}q} H(\phi)\,\mathrm{d}x. \tag{10}$$

$$\frac{\mathrm{d}F}{\mathrm{d}q_2} = \int_\Omega \frac{\mathrm{d}F}{\mathrm{d}q}\frac{\mathrm{d}q}{\mathrm{d}q_2}\,\mathrm{d}x = \int_\Omega \frac{\mathrm{d}F}{\mathrm{d}q}(1 - H(\phi))\,\mathrm{d}x, \tag{11}$$

where δ is the Dirac delta function.

We will use the method of gradient descent to solve the minimization problem. More precisely, we will consider the following iterative scheme for ϕ, q_1 and q_2:

$$\phi^{k+1} = \phi^k - \alpha_k \frac{\mathrm{d}F}{\mathrm{d}\phi}(\phi^k, q_1^k, q_2^k), \tag{12}$$

$$q_j^{k+1} = q_j^k - \gamma_k^j \frac{\mathrm{d}F}{\mathrm{d}q_j}(\phi^{k+1}, q_1^k, q_2^k), \quad j = 1,2. \tag{13}$$

The step sizes $\alpha_k > 0$ and $\gamma_i^k > 0$ can be fixed during all the iterations or be obtained by line search. However, in all of the following numerical tests, we use line search for α_k and γ_k^j ($j = 1,2$). Precautions have to be taken when conducting numerical calculations with the delta function $\delta(\phi)$ and the Heaviside function $H(\phi)$. They are, in a more precise sense, limits of C^∞ functions. One way to tackle this problem is to replace the delta function $\delta(\phi)$ and the Heaviside function $H(\phi)$ by using the following smooth approximations:

$$\delta_\epsilon(\phi) = \frac{\epsilon}{\pi(\phi^2 + \epsilon^2)}, \tag{14}$$

$$H_\epsilon(\phi) = \frac{1}{\pi}\tan^{-1}\left(\frac{\phi}{\epsilon}\right) + \frac{1}{2}, \tag{15}$$

with $\epsilon > 0$ chosen to be the order of the mesh size. See [8,39].

During the iteration procedure according to (12) for the function ϕ, the new iterate may not be a signed distance function anymore. In this reconstruction algorithm (12), (13), only the sign of the function ϕ is important and the value of the function ϕ is irrelevant. So, as the iteration for ϕ proceed, we would like to replace the new iterate by a signed distance function so that it has the same sign as the corresponding iterate. This can be done by solving (6). In all of the experiment below, this replacement is done when the function ϕ is changed by 10% measured in relative L^2-norm.

3. Numerical tests

This section aims at showing the usefulness of the numerical scheme derived in previous section. A series of numerical experiments were carried out in order to confirm numerically that the scheme is able to recover simultaneously the material interface and conductivity coefficient values in some situations which appear often in practice.

For ease of exposition, we set $\Omega = [0,1]^2$. We will triangulate the domain by dividing it into uniform squares with side length h. Each square is then divided into two triangles by cutting along one of its diagonals. As a result, we have a set of triangles triangulating the domain Ω. In all of the following examples, we take $h = 1/16$. Furthermore, we will always use dash lines to represent the numerical computed interface while use solid lines to represent the true interface.

The data for the potential u on the boundary are generated in the following manner. We set u equals 1 on one of the four sides of the rectangular domain Ω and 0 elsewhere. So, we have a set of four data in this form. Next, we divide each side of Ω into two parts. Then, we set u equal 1 on one part and 0 on the other part, while setting u equal 0 on the other three sides. So, we have a set of eight data in this form. Next, we divide each side into four parts and set u equals one on one part and zero on the other three parts. Then, we get a set of 16 data in this form. Hence, by continuing in this manner, we have a set of 4, 12, 28 and 60 data, respectively.

We will also add some uniform noise to the data and the data are generated on a finer mesh using the true solutions. We use the relative error in the L^2-norm on the boundary to measure the noise level in the data.

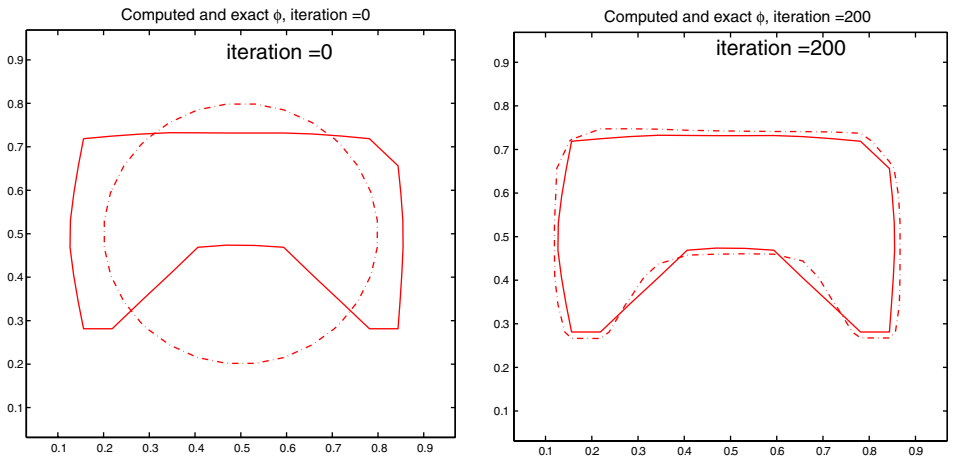

Fig. 1. Left picture shows the initial guess. Right picture shows the numerical result after 200 iterations.

The regularization parameter is chosen experimentally. A few values are used to solve a particular problem. Then we choose the one that gives the best numerical result. We remark here that an even better way of choosing the regularization parameter is to employ the discrepancy principle [41].

3.1. Simultaneous reconstruction

In this example, we use 60 measurement data with 0.05% noise. The regularization parameter β is chosen to be 10^{-7}. The true conductivity value is 1 inside the region enclosed by the solid line and is 10 outside. We will fix $q_2 = 10$ during the iterations. We pick a circle, shown in dash line in the left picture in Fig. 1, as our initial guess for the material interface. Also, we pick an initial guess for the conductivity coefficient to be 1.1 inside. The numerical result after 200 iterations is shown in Fig. 1. At convergence, the conductivity $q_1 = 1.3$ inside.

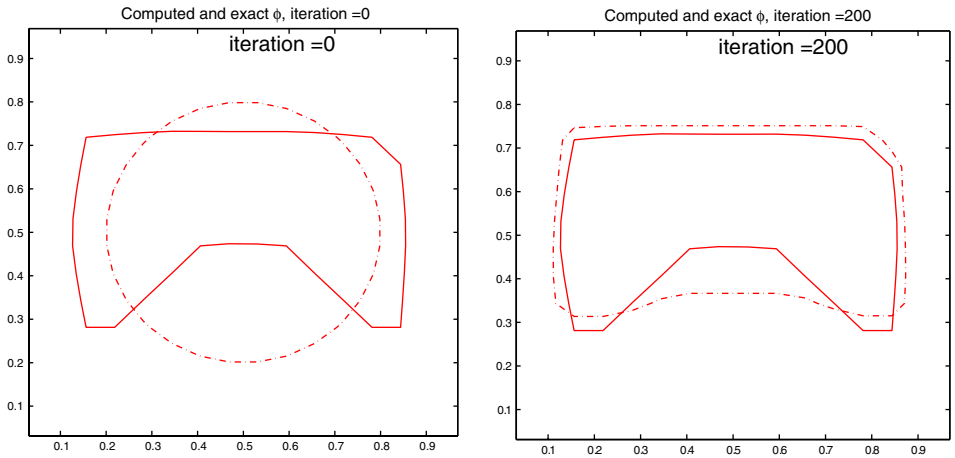

Fig. 2. Left picture shows the initial guess. Right picture shows the numerical result after 200 iterations.

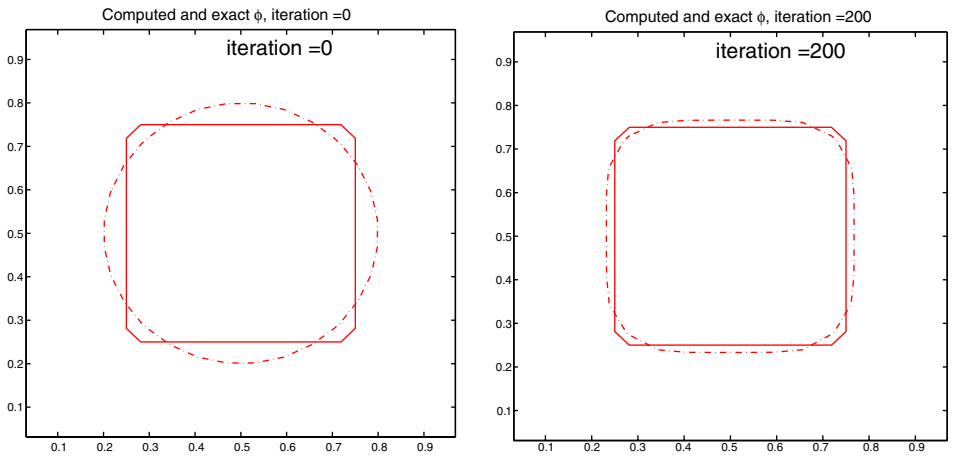

Fig. 3. Left picture shows the initial guess. Right picture shows the numerical result after 200 iterations.

We see that, in the presence of 0.05% noise in the measurement data, our numerical scheme can almost recover the shape of the unknown interface. Furthermore, we see that we can recover the geometry of the unknown interface without knowing much about it, as can be seen from our choice of the initial guess which contains no information about the true interface.

Next, we will consider the same example as above but with different noise level. We add, in this case, 0.1% noise in the data. We also change the regularization parameter to 10^{-6} due to the larger noise. Fig. 2 shows the numerical result after 200 iterations. The recovered value of the conductivity coefficient inside the region is 1.8.

We next consider an example with a different shape. We again use 60 measurements, 0.1% noise in the data and $\beta = 10^{-6}$. The true conductivity value is again 1 inside the region enclosed by the solid line and is 10 outside. The initial guess for the value inside the region is 1.1. Fig. 3 shows the initial guess for the interface and the numerical solution of the interface at 200 iterations.

In this experiment, the recovered value of the conductivity inside the region is 1.3. From this numerical test, we see that our numerical algorithm can accurately recover the material interface even in the presence of 0.1% noise in the data.

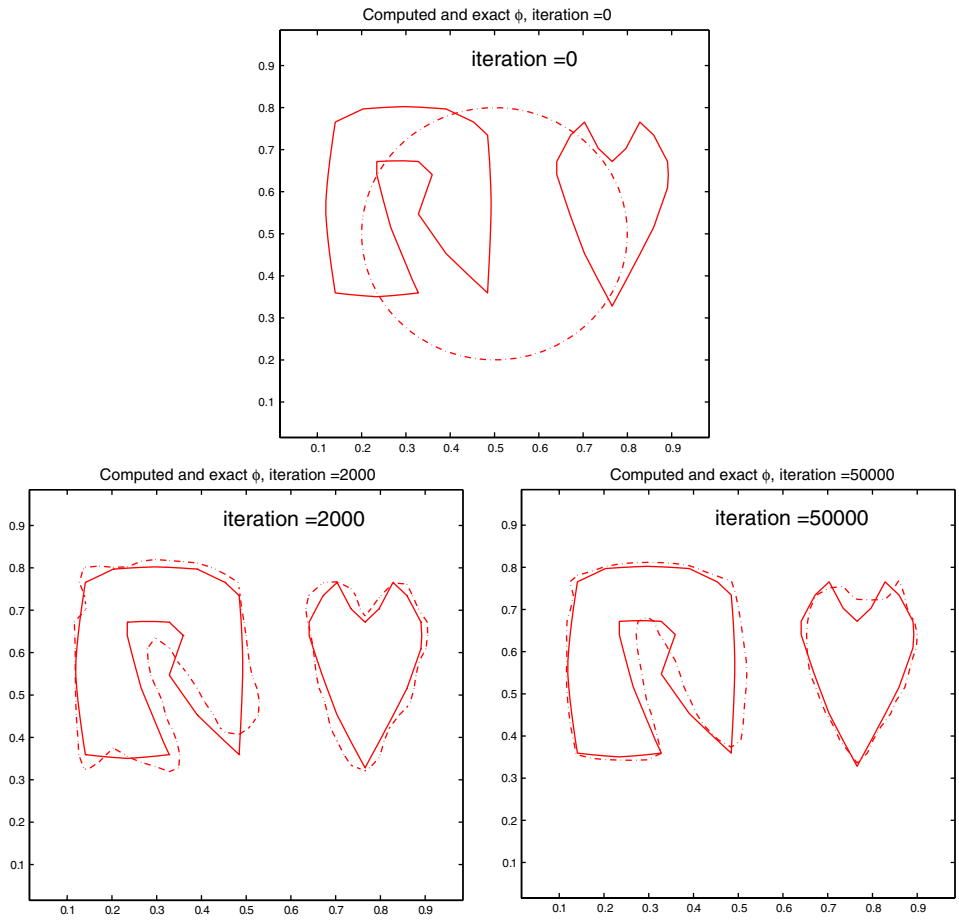

Fig. 4. Results with no noise in the data. Up: initial guess. Left: numerical solution after 2000 iterations with computed $q = 2.129$. Right: numerical solution after 50,000 iterations with computed $q = 1.789$.

We next consider an example with an object with a more complicated geometry. We will first test the algorithm with no noise in the given data. We take 60 measurements and set the regularization parameter β to be 10^{-12}. We decrease the mesh size to $h = 1/32$. The true value of the conductivity coefficient is 1 inside the region and is 10 outside the region. The initial guess for the value inside the region is 1.1. Fig. 4 shows the initial guess of the interface and the numerical solution after 2000 and 50,000 iterations. From the results in Fig. 4, we see that relatively few iterations are needed to capture the material interface with good accuracy. However, more iterations are needed in order to get better accuracy of the recovered value of the conductivity coefficient as a result of the ill-posedness of the problem. Fig. 5 shows numerical results of the same example with 0.01% noise in the data.

In the following, we present the results of an example with the mesh size decreased to $h = 1/64$. From Fig. 6, we see that the concave part of the object can be more accurately recovered. Moreover, the recovered value of the conductivity coefficient is more accurate.

In the last example of this section, we present a result of an example with the initial guess of the value of the conductivity coefficient inside the region to be $q = 3$ instead of $q = 1.1$. We will set the mesh size $h = 1/32$

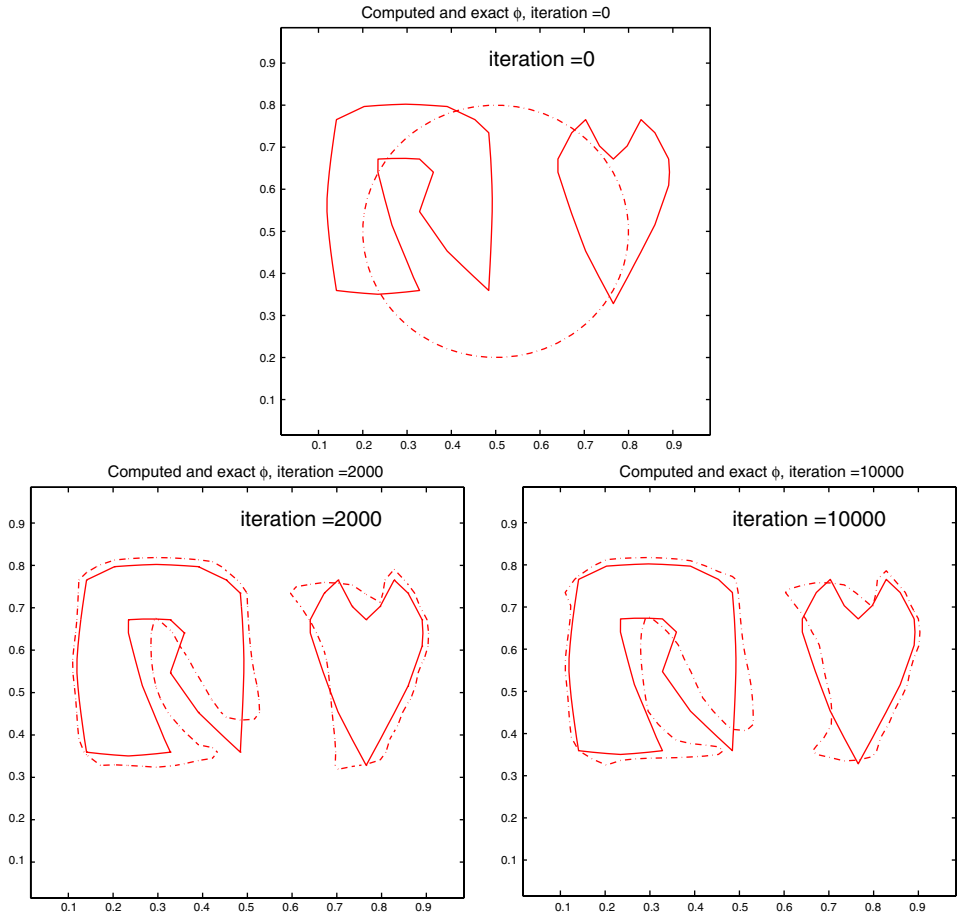

Fig. 5. Results with 0.01% noise in the data. Up: initial guess. Left: numerical solution after 2000 iterations with computed $q = 2.092$. Right: numerical solution after 10,000 iterations with computed $q = 1.941$.

in this case. From Fig. 7, we see that the material interface can be recovered even though the initial value of q is far away from the true value. In addition, the recovered value of q is 2.273.

3.2. Sensitivity on number of observations

In this section, we will see the effect of the number of observations on the accuracy of the numerical solution. Here, we take the regularization parameter β to be 10^{-8} and we also add 1% noise in the data. To see the effect, we perform four different numerical calculations of a known interface by using 4, 12, 28 and 60 measurements. Fig. 8 shows an initial guess for our method. The numerical results are shown in Fig. 9. The upper left, upper right, lower left and lower right figures show results with 4, 12, 28 and 60 measurements, respectively. From the numerical results above, we see that, as the number of measurements increases, we have a better accuracy of the unknown interface. When the number of measurement is 60, we almost re-

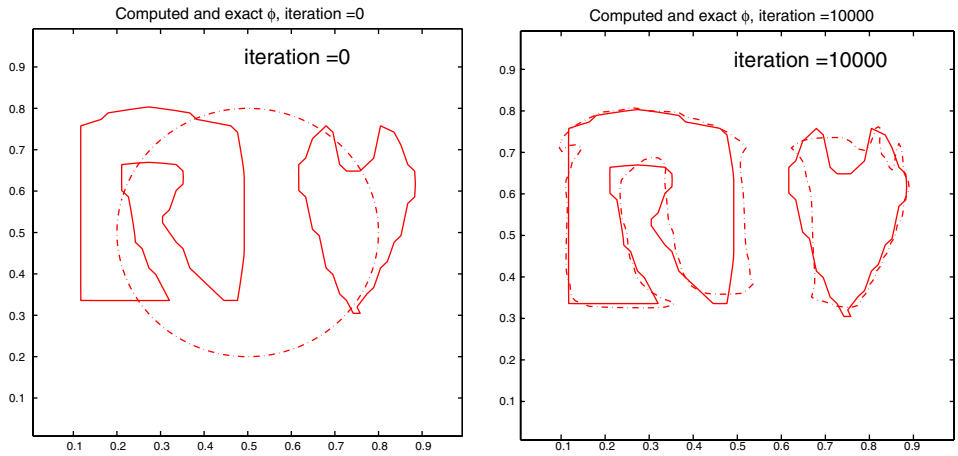

Fig. 6. Result with 0.01% noise in the data. Left: initial guess. Right: numerical result after 10,000 iterations with computed $q = 1.599$.

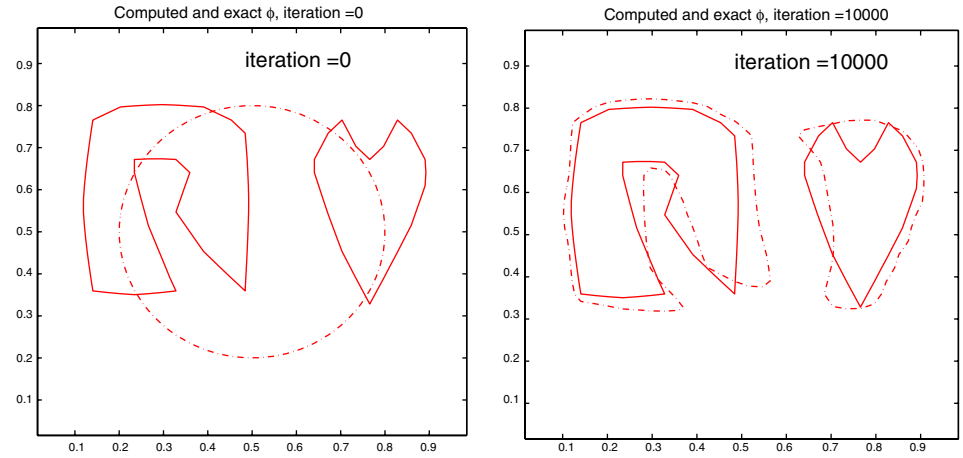

Fig. 7. Result with 0.01% noise in the data. Left: initial guess. Right: numerical result after 10,000 iterations with computed $q = 2.273$.

cover the exact interface. In addition, even with a very small number of measurement (e.g., 4) we can still roughly get the shape of the unknown interface. From this numerical experiment, we see that the concave portion of the unknown object is more difficult to be recovered than other part where the object is convex.

3.3. Sensitivity on noise level

In this section, we will see the effect of the noise on the computational results. We will test our algorithm against different noise levels. Here, we fix the number of measurements to be 60. We will perform four numerical tests with noise ranging from 1% to 4%. The true interface in this case is a square sitting in the middle of the domain Ω. We pick an initial guess for the numerical scheme to be a circle sitting in the middle of the domain (see Fig. 10). In Fig. 11, we show the numerically computed interfaces with different noise levels. The upper left, upper right, lower left and lower right figures show the numerically computed interface with 1%, 2%, 3% and 4% of noise in the data, respectively. The corresponding regularization parameter β are 10^{-13}, 10^{-10}, 2×10^{-6} and 5×10^{-5}, respectively. We see that our numerical algorithm can, at least, tolerate noise level up to 4%. Also, at this noise level, our algorithm can produce quite accurate result.

3.4. Sensitivity on regularization parameter

In this section, we will demonstrate the effect of the choice of the regularization parameter β. We fix the number of measurements to be 60. The true interface is a circle sitting in the middle of the domain (see Fig. 12). The initial guess is chosen to be a circle with the same center as that of the true interface and smaller radius.

We show the results with different regularization parameters in Fig. 13. The upper left, upper right, lower left and lower right figures show the results with the regularization parameter is chosen to be 10^{-4}, 10^{-5}, 10^{-6} and 10^{-7}, respectively. The corresponding noise levels in the data are 7%, 2%, 1% and 0.5%, respectively. From this numerical experiment, we see that the choice of the regularization parameter is crucial to the success of our numerical scheme. The general principle is the higher the noise level, the greater the regularization parameter should be used. In this particular experiment, when the regularization parameter is chosen to be 10^{-4}, the numerical scheme can recover the true interface with noise level up to 7%. On the

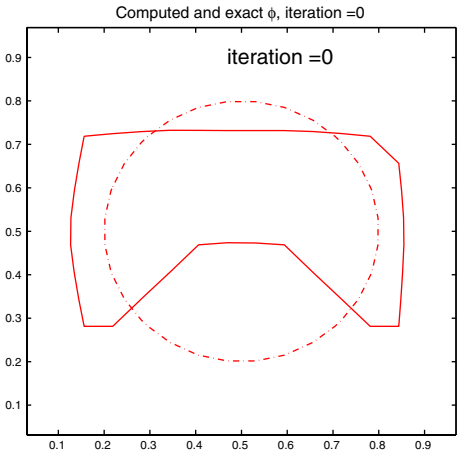

Fig. 8. A circle is chosen to be an initial guess.

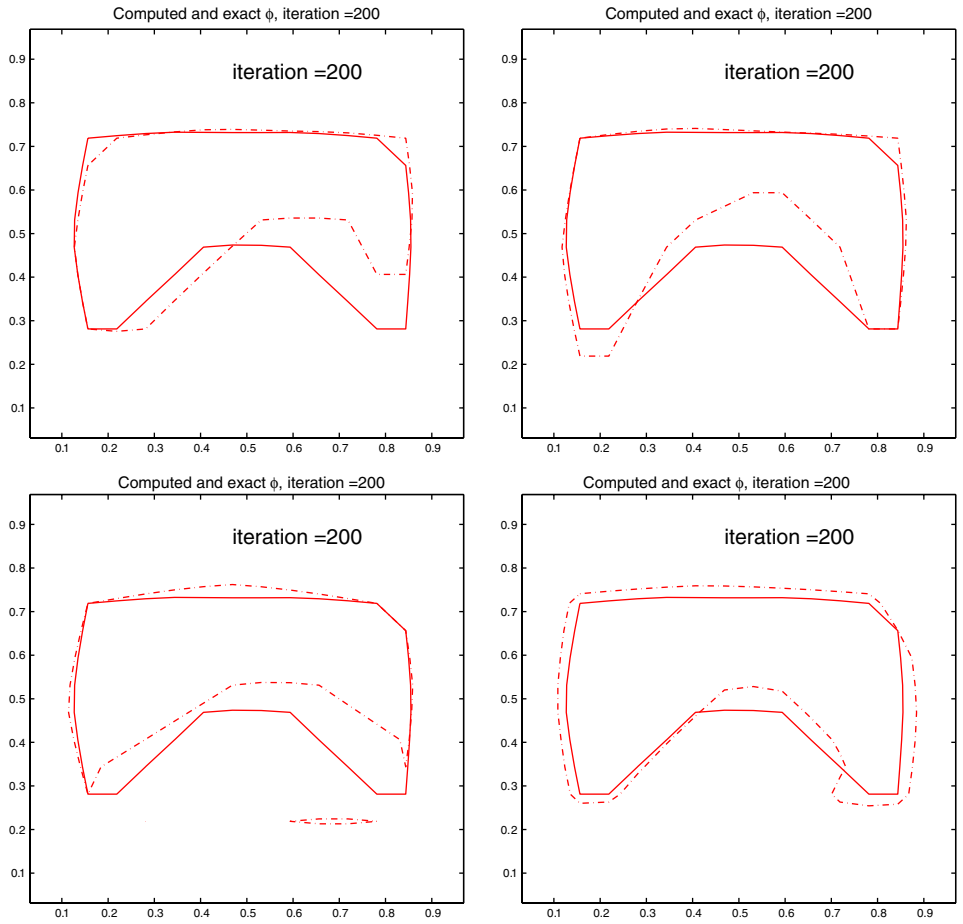

Fig. 9. The upper left, upper right, lower left and lower right figures show results with 4, 12, 28 and 60 measurements.

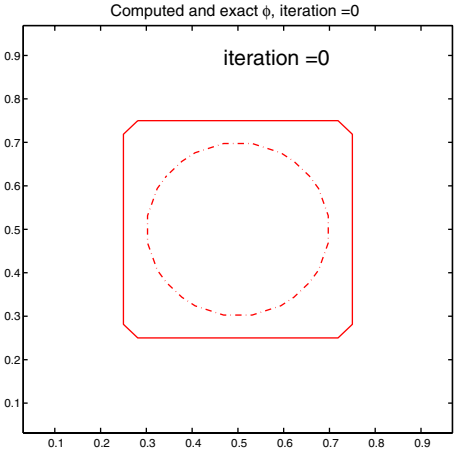

Fig. 10. A circle is chosen to be an initial guess.

other hand, when the regularization parameter is chosen to be 10^{-7}, the numerical scheme can only recover the true interface with noise level up to 0.5%. In addition, as the value of the regularization parameter increases, the numerical scheme can tolerate higher level of noise in the data.

3.5. Comment on computational efficiency

The problem of identifying both the material interface and the value of the coefficient is highly ill-posed. As shown in the numerical examples from Figs. 4 and 5, we see that relatively few iterations are needed to capture the material interface with good accuracy. However, more iterations are needed in order to get better accuracy of the recovered value of the conductivity coefficient as a result of the ill-posedness of the problem.

There are many ways to improve the speed. All the equations for the forward and the adjoint problems have the same matrices with different right-hand sides. Moreover, very good initial values are available for these problems during the iterations. Thus, some fast methods can be used to solve the forward and adjoint

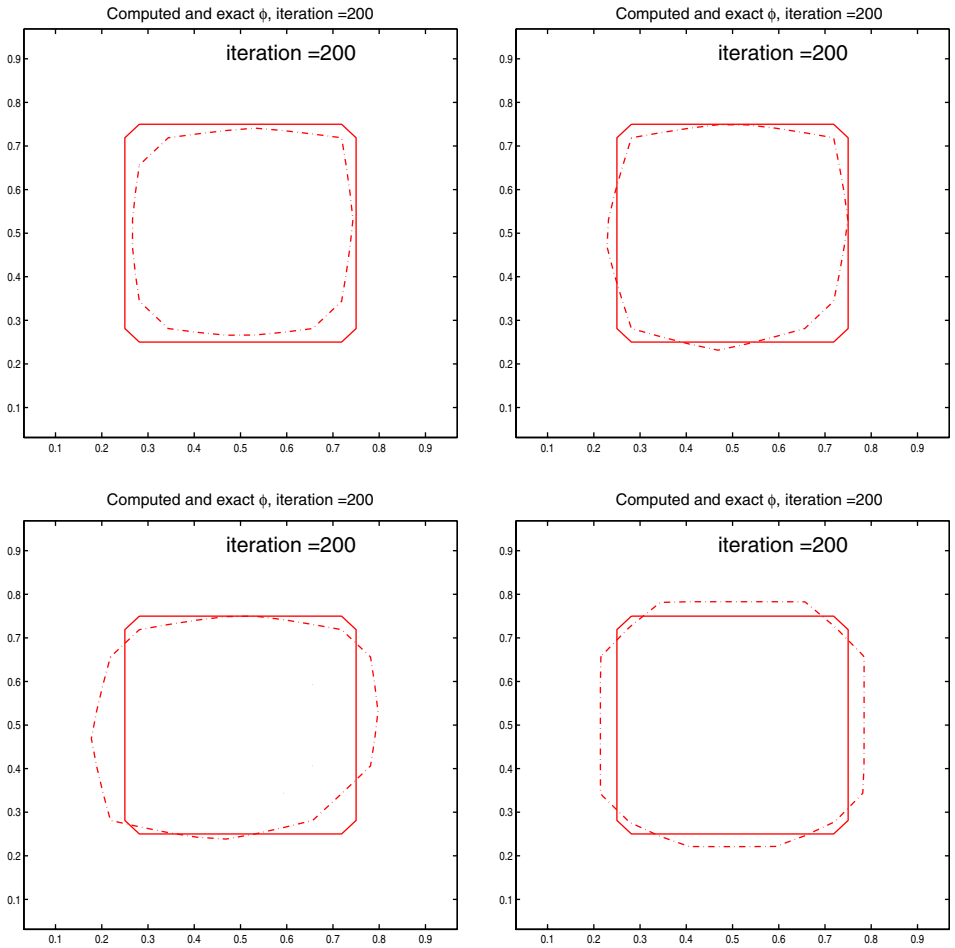

Fig. 11. The upper left, upper right, lower left and lower right figures show results with 1%, 2%, 3% and 4% noise and regularization parameter 10^{-13}, 10^{-10}, 2×10^{-6} and 5×10^{-5}, respectively.

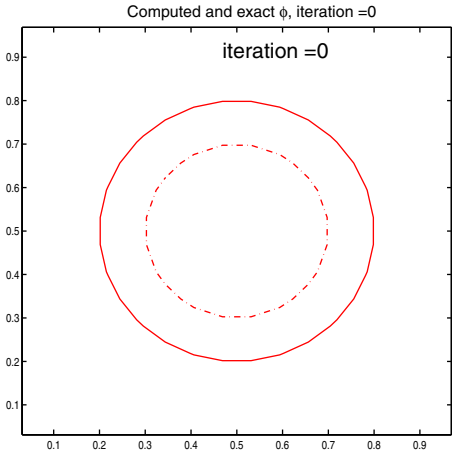

Fig. 12. A circle is chosen to be an initial guess.

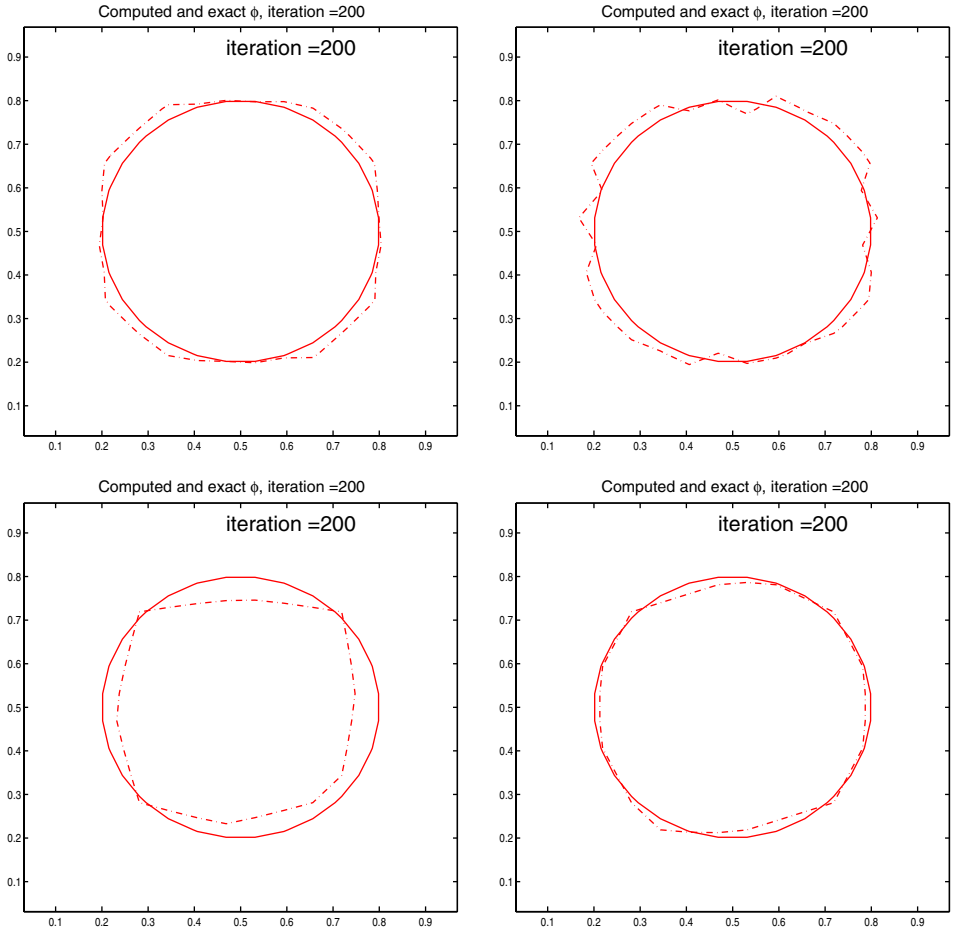

Fig. 13. The upper left, upper right, lower left and lower right figures show results with the regularization parameter chosen to be 10^{-4}, 10^{-5}, 10^{-6} and 10^{-7} and noise level 7%, 2%, 1% and 0.5%, respectively.

problems. The gradient decent method used here is very slow, but rather stable. We could combine the gradient decent method with the Newton method and that will reduce the iteration number a lot. Other computationally more efficient methods are certainly possible but are beyond the scope of our current paper.

4. Conclusion

For electrical impedance tomography, it is sometimes more important to recover the shape of the domains containing different materials than to recover the values for the materials. Level set methods are natural choices for this kind of applications. In this work, we have demonstrated that level set methods can produce rather good results in identifying the sharp interfaces in the presence of noise in the observation data. In order to use this approach for practical problems, we need to improve the efficiency of the algorithms. More efficient level set minimization algorithms shall be tested [36]. An efficient algorithm for solving the forward problems would also improve a lot of the numerical performances of the proposed algorithms.

Acknowledgments

We acknowledge support from the ONR under Grant N00014-96-1-0277, from the NSF under contract DMS-9973341 and from the NIH under Grant P20MH65166.

References

[1] A. Allers, F. Santosa, Stability and resolution analysis of a linearized problem in electrical impedance tomography, Inverse Problems 7 (4) (1991) 515–533.
[2] H.B. Ameur, M. Burger, B. Hackl, On some geometric inverse problems in linear elasticity, UCLA, Mathematics Department, CAM-Report 03-35, 2003.
[3] M. Brühl, Explicit characterization of inclusions in electrical impedance tomography, SIAM J. Math. Anal. 32 (2001) 1327–1341.
[4] M. Brühl, M. Hanke, Numerical implementation of two noniterative methods for locating inclusions by impedance tomography, Inverse Problems 16 (2000) 1029–1042.
[5] M. Burger, A level set method for inverse problems, Inverse Problems 17 (2001) 1327–1356.
[6] M. Burger, Levenberg–Marquardt level set methods for inverse obstacle problems, UCLA, Mathematics Department, CAM-Report 03-45, 2003.
[7] M. Burger, A framework for the construction of level set methods for shape optimization and reconstruction, Interfaces Free Boundaries 5 (2003) 301–329.
[8] T.F. Chan, X.-C. Tai, Level set and total variation regularization for elliptic inverse problems with discontinuous coefficients, J. Comput. Phys. 193 (2003) 40–66.
[9] T.F. Chan, X.-C. Tai, Identification of discontinuous coefficients from elliptic problems using total variation regularization, SIAM J. Sci. Comp. 25 (2003) 881–904.
[10] M. Cheney, D. Isaacson, J.C. Newell, Electrical impedance tomography, SIAM Rev. 41 (1999) 85–101 (electronic).
[11] M. Cheney, D. Isaacson, J. Newell, J. Goble, S. Simske, NOSER: an algorithm for solving the inverse conductivity problem, Int. J. Imaging Syst. Technol. 2 (1990) 66–75.
[12] A. Dey, H.F. Morrison, Resistivity modeling for arbitrarily shaped three dimensional structures, Geophysics 44 (1979) 753–780.
[13] D.C. Dobson, F. Santosa, An image-enhancement technique for electrical impedance tomography, Inverse Problems 10 (2) (1994) 317–334.
[14] D.C. Dobson, F. Santosa, Resolution and stability analysis of an inverse problem in electrical impedance tomography: dependence on the input current patterns, SIAM J. Appl. Math. 54 (6) (1994) 1542–1560.
[15] O. Dorn, E.L. Miller, C.M. Rappaport, A shape reconstruction method for eletromagnetic tomography using adjoint and level sets, Inverse Problems 16 (2000) 1119–1156.

[16] M. Ikehata, S. Siltanen, Numerical method for finding the convex hull of an inclusion in conductivity from boundary measurements, Inverse Probl. 16 (4) (2000) 1043–1052.
[17] K. Ito, K. Kunisch, Z. Li, Level-set function approach to an inverse interface problem, Inverse Probl. 17 (2001) 1225–1242.
[18] S. Jarvenpaa, E. Somersalo, Impedance imaging and electrode models, in: Engl, W. Heinz et al. (Eds.), Inverse Problems in Medical Imaging and Nondestructive Testing, Proceedings of the Conference in Oberwolfach, Germany, February 4–10, 1996, Springer, Wien, 1997, pp. 65–74.
[19] J.P. Kaipio, V. Kolehmainen, E. Somersalo, M. Vauhkonen, Statistical inversion and Monte Carlo sampling methods in electrical impedance tomography, Inverse Probl. 16 (5) (2000) 1487–1522.
[20] V. Kolehmainen, S.R. Arridge, W.R.B. Lionheart, M. Vauhkonen, J.P. Kaipio, Recovery of region boundaries of piecewise constant coefficients of an elliptic PDE from boundary data, Inverse Probl. 15 (5) (1999) 1375–1391.
[21] Y. Li, D.W. Oldenburg, Inversion of 3-d dc resistivity data using an approximate inverse mapping, Geophys. J. Int. 116 (3) (1994) 557–569.
[22] J. Lie, M. Lysaker, X.-C. Tai, A variant of the level set method and applications to image segmentation, UCLA CAM Report 03-50, 2003. Available from: <http://www.math.ucla.edu/applied/cam>.
[23] W.R.B. Lionheart, Conformal uniqueness results in anisotropic electrical impedance imaging, Inverse Probl. 13 (1) (1997) 125–134.
[24] W.R.B. Lionheart, Boundary shape and electrical impedance tomography, Inverse Probl. 14 (1) (1998) 139–147.
[25] W.R.B. Lionheart, EIT reconstruction algorithms: pitfalls, challenges and recent developments, physiological measurement, to appear. Available from: <http://www.arxiv.org/abs/physics/0310151>.
[26] P.R. McGillivray, Forward modelling and inversion of DC resistivity and MMR data, Ph.D. Thesis, University of British Columbia, 1992.
[27] S.J. Osher, M. Burger, E. Yablonovitch, Inverse problem techniques for the design of photonic crystals, UCLA, Mathematics Department, CAM-Report 03-31, 2003.
[28] S.J. Osher, R.R. Fedkiw, Level set methods: an overview and some recent results, J. Comput. Phys. 169 (2) (2001) 463–502.
[29] S.J. Osher, F. Santosa, Level set methods for optimization problems involving geometry and constraints. I. Frequencies of a two-density inhomogeneous drum, J. Comput. Phys. 171 (2001) 272–288.
[30] S.J. Osher, J.A. Sethian, Fronts propagating with curvature dependent speed: algorithms based on Hamilton–Jacobi formulations, J. Comput. Phys. 79 (1988) 12–49.
[31] L. Rondi, F. Santosa, Enhanced electrical impedance tomography via the Mumford–Shah functional, Control, optimisation, and calculus of variations, to appear. Available from: <http://www.math.umn.edu/%7Esantosa/fs.html>.
[32] F. Santosa, M. Vogelius, A backprojection algorithm for electrical impedance imaging, SIAM J. Appl. Math. 50 (1) (1990) 216–243.
[33] S. Siltanen, J. Mueller, D. Isaacson, An implementation of the reconstruction algorithm of A. Nachman for the 2D inverse conductivity problem, Inverse Probl. 16 (3) (2000) 681–699.
[34] N.C. Smith, K. Vozoff, Two dimensional DC resistivity inversion for dipole dipole data, IEEE Trans. Geosci. Remote Sensing GE 22 (1984) 21–28 (special issue on electromagnetic methods in applied geophysics).
[35] E. Somersalo, M. Cheney, D. Isaacson, Existence and uniqueness for electrode models for electric current computed tomography, SIAM J. Appl. Math. 52 (4) (1992) 1023–1040.
[36] B. Song, T.F. Chan, Fast algorithm for level set segmentation, UCLA CAM Report 02-68, 2002.
[37] A. Tamburrino, G. Rubinacci, A new non-iterative inversion method for electrical resistance tomography, Inverse Probl. 18 (6) (2002) 1809–1829.
[38] A. Tamburrino, S. Ventre, G. Rubinacci, Electrical resistance tomography: complementarity and quadratic models, Inverse Probl. 16 (5) (2000) 1585–1618.
[39] L.A. Vese, T.F. Chan, A new multiphase level set framework for image segmentation via the Mumford and Shah model, Int. J. Comput. Vision 50 (3) (2002) 271–293.
[40] L. Vese, S. Osher, The level set method links active contours, Mumford–Shah segmentation, and total variation restoration. CAM Report 02-05, UCLA Mathematics Department, 2002.
[41] C. Vogel, Computational Methods for Inverse Problem, SIAM, Philadelphia, 2001.
[42] W.P. Ziemer, Weakly Differentiable Functions, Springer, Berlin, 1989.